IEEE Access
Multidisciplinary | Rapid Review | Open Access Journal

Received September 29, 2020, accepted October 13, 2020, date of publication October 20, 2020, date of current version November 3, 2020.

Digital Object Identifier 10.1109/ACCESS.2020.3032458

Model Free Traveling Wave Based Fault Location Method for Series Compensated Transmission Line

O. D. NAIDU[1], (Senior Member, IEEE), AND ASHOK KUMAR PRADHAN[2], (Senior Member, IEEE)

[1]Hitachi ABB Power Grids Research and Development Center, Bengaluru 560048, India
[2]Department of Electrical Engineering, Indian Institute of Technology, Kharagpur 721302, India

Corresponding author: O. D. Naidu (od.naidu@hitachi-powergrids.com)

ABSTRACT Locating fault position in a series compensated transmission line is a difficult task due to the non-linear characteristics of the metal-oxide varistor which is present in the protection system of the compensator. In this paper, a model-free two-terminal traveling wave-based fault location method for a series compensated line is proposed. The technique makes use of two subroutines which calculate the fault locations assuming that the fault position to be on the left and right side of the series compensator respectively. The method then selects the correct fault location of the two by a special logic based on faulted half-section identification. The first two traveling wave arrival times recorded at both the terminals of the line are used in the method. The proposed technique does not require model information of the series capacitor and transmission line. It has been verified using the PSCAD/EMTDC model of a 400-kV, 300 km transmission line which is compensated by a fixed series capacitor in the middle and line ends. The performance of the proposed method is compared with a commercially available classical two-ended techniques and setting-free method.

INDEX TERMS Faulted half-section identification, series compensated lines, synchronized data, traveling-wave-based fault locator.

I. INTRODUCTION

To meet the growing power demand, utilities have widely installed series capacitors on long transmission lines [1]. The main purpose of series compensation in power systems is a virtual reduction of the line reactance to enhance the power system stability, damping of the power system oscillations, better controllability of the power flow, and enhance the power transfer capability of transmission corridors [1]. However, the protection and fault location (FL) for series compensated line (SCL) is one of the most difficult tasks of the intelligent electronic device (IED) manufacturers and utility protection engineers due to the non-linear characteristics of the series capacitor protection unit (Metal Oxide Varistor (MOV)) [1]–[4] in the measurement loop.

Faults are inevitable in transmission lines due to natural events such as storms, lightning, snow, rain, insulation breakdown, and other causes such as birds, tree branches, and other external objects [4]. Quick restoration of service could reduce customer complaints, outage time, revenue loss for the utilities [4], [5]. Restoration of power supply following a permanent fault can be done only after the maintenance team finishes the repair of the damage caused by the fault. For this purpose, the FL is to be known, otherwise, the whole line is to be inspected. Thus, it is important that the location of a fault needs to be known with good accuracy. FL for a series compensated line is one of the most crucial tasks for the IED manufacturers and utility maintenance staff since such lines usually spread over a few hundreds of kilometers.

FL techniques are mainly classified into three categories [5]; impedance, traveling wave (TW), and artificial intelligence-based techniques. Impedance-based FL techniques are traditionally used by transmission utilities because of simplicity and require low hardware cost [4]–[6]. Various impedance-based FL methods are proposed for SCLs [8]–[15]. However, the precision of impedance-based FL techniques [4] is influenced by fault resistance, system non-homogeneity, measurement transformers

The associate editor coordinating the review of this manuscript and approving it for publication was Pietro Varilone.

inaccuracies [6], [7], and phasor estimation accuracy [14]. A fault on SCL introduces a sub-synchronous frequency component along with a decaying dc component in the measured fault signal. With such signal modulation, estimated phasors will be oscillatory and erroneous [14], [15] and therefore such a method has limited performance scope for SCLs. Compared to impedance-based FL techniques [8]–[15], TW-based techniques [16]–[28] are better suited for SCLs as FL accuracy depends on the time of arrival of TWs and wave speed. These methods are immune to various fault situations and independent of installed equipment.

Two-ended TW based techniques are extremely precise and reliable to locate the fault on the transmission lines [16], [17] than the single-ended methods [18], [19]. The single-ended methods pose difficulty in distinguishing the waves reflected from the fault and the remote terminals, as well as the waves reflected from the buses of adjacent short lines connected to the monitored line [19]. Several two-ended techniques are reported in the literature [16], [17] and [20]–[27]. Two ended TW based FL technique based on synchronized data [16], [17], electromagnetic time-reversal [20], wide area measurement [21], distributed current sensing [22] and unsynchronized data [23]–[25] are reported for uncompensated transmission lines.

Two-ended synchronized data-based fault detection and location are presented for SCLs in [26] and [27]. Single-ended TW based FL for series compensated technique is presented in [28] using voltage and current measurements. The fault locator is placed at the compensator and this method requires the voltage and current measurements at the middle of the line (i.e. at compensator) and this method may not be economical for practical deployment. The accuracy of the reported two ended methods [16], [17], [20]–[27] highly depends on the wave speed (line parameters such as inductance and capacitance per unit length). These line parameters may not be correct always and depend on many practical conditions such as weather, age of the conductor, temperature and sag, etc. The online estimation of line parameters accurately is challenging with series compensation [29] due to voltage and current inversions as well as the presence of low-frequency oscillations during faults on lines close to the capacitors [30]. Therefore, the FL accuracy with the techniques as in [16], [17] and [20]–[27] may not be good enough for SCLs. The wave speed adjustment by creating faults at a known distance is available in [31]. For example, with one end of the line open, energize the line from the remote end and then capture the TW arrival time and calculate the wave speed based on the known length of the line. This technique requires an experiment to obtain the wave speed which is a time-consuming procedure and not economical.

Setting-free phasor-based FL method for three-terminal lines is presented in [32] using all terminal data and it may not be suitable to SCL [4]. The FL is obtained by solving the non-linear equations and which requires high computation burden. Incremental quantity-based fault section identification (FSI) for SCL is presented [33] and the accuracy of FSI is influenced by fault resistance and a source impedance of the line. Setting-free TW-based FL method has been reported in [34] which requires both ground and aerial mode signals. The ground mode signals are highly attenuated and available only for earth faults. A distributed TW-based FL technique that uses measurements at three locations of the line is proposed in [35] which does not require wave speed. It requires measurement devices to be installed at three locations on the line and therefore not cost-effective. A method to avoid the limitation of wave speed (line parameters) is available in [36] for uncompensated lines. However, this method requires a proper initial guess of the wave speed and approximate latency information of the communication channel. Further, this is a search-based method and depends on the time difference between the first incident TW and the one reflection from the fault point, at both the terminals of the line. The technique may find limited performance for faults close to the terminals of the line due to the requirement of TW arrival times of incident and reflection waves from the fault point, at both ends. Online parameter computation of SCLs being difficult due to non-linear characteristics of MOV present in the measurement loop, there is a scope to find an accurate *model-free* FL technique for series compensated lines.

In this paper, a model-free FL method for series compensated transmission lines using two ended synchronized current measurements is proposed. In the approach, two fault location subroutines are used by assuming the fault to be on the left and right sides of the series compensator respectively. Correspondingly, for one fault case, two FLs are calculated using the first two TW arrival times measured at both the terminals. Then the correct fault distance is selected from the two using the faulted half-section identification (FHI) information. The faulted half-section (FH) is determined by comparing two indices computed using TW arrival times recorded at both the terminals. The first FHI index is obtained by taking the difference between the second TW arrival time recorded at a remote terminal and the first arrival time recorded at the local terminal of the line. The second FHI index is calculated by taking the difference between the second TW arrival time recorded at the local terminal and the first arrival time measured at the remote terminal of the line.

The method does not require information of line parameters (or wave speed), compensation level at an instant, or MOV model parameters. Accuracy of the proposed technique depends solely on the sampling rate of the data acquisition system and the precision of TW arrival time calculation. The proposed FL method can be used for any line, including SCL. The main contributions of this work are as follows:

(i) novel model-free fault location formulation which does not require line parameters (or wave speed) and the formulation also eliminates the effect of TW dispersion [37], [38] on FL accuracy and (ii) identification of faulted half-section using TW arrival times.

In recent developments, power companies are deploying the cloud-based platform, as part of their digitalization

program [39]. Fault location is one of the applications therein which can be calculated by uploading the disturbance recorder data into the cloud from stations. The final FL information is then sent to the field staff for faster restoration [39]. The proposed method is amenable to such new digital deployment; an added advantage over available FL methods. Being model-free, the proposed solution is advantageous for practical deployment [39], even using such an emerging technology. Further, once the fault location is known, the method can produce an accurate estimate of the wave speed of the line for any other possible applications. The proposed technique is verified through the PSCAD/EMTDC simulations covering various fault scenarios for 400-kV, 300 km line with series compensation at middle and line ends, and found to be accurate. The method is also tested with field fault data collected from a 400-kV, 225km double circuit SCL [40], [41] in Indian Power Grid between Jeypore-Gazuwaka substations.

II. PROPOSED METHOD

The proposed technique uses four functional modules: (i) the model-free fault location formulation and (ii) the faulted half-section identification logic, (iii) effect of the location of the series capacitor and level of compensation, and (iv) illustrative of the application of the proposed method. These modules can be implemented in an intelligent electronic device (IED) platform with a signal sampling frequency of 1 MHz. The details of the modules are provided below.

A. PROPOSED MODEL-FREE FAULT LOCATION FORMULATION

Consider a SCL connecting to terminal A and B as shown in Fig.1 (a) where the compensator is at the middle of the line. The fault locator is placed at terminal A. The current measurements from both the terminal are available to the fault locator. Various traveling wave detection and extraction methods are available in the literature and this paper is not focused on the process of traveling wave detection and extraction. Traveling waves are extracted using a bandpass filter and the steps are described in [16] and the same process is adopted in this work. The TWs are extracted from the current signal and the first two TW arrival times are used to achieve model-free FL and FHI. Two fault cases are considered (i) fault on the left side of the compensator (first half-section of the line) and (ii) fault on the right side of the compensator (second half-section of the line).

1) FAULT ON THE LEFT SIDE OF THE SERIES COMPENSATOR

Consider a fault ($F1$) in the first half ($0 < d_1 < l_{AB}/2$) of the line (length of the line be l_{AB} km). For the case, the corresponding lattice diagram is shown in Fig.1(b). Note that no TW reflections and refractions from the compensator due to no impedance change at the capacitor [42] during the first few milliseconds after the fault. From the lattice diagram, we can write,

$$t_{A1} = t_{0A} + \frac{\mathrm{d}_1}{v} \tag{1}$$

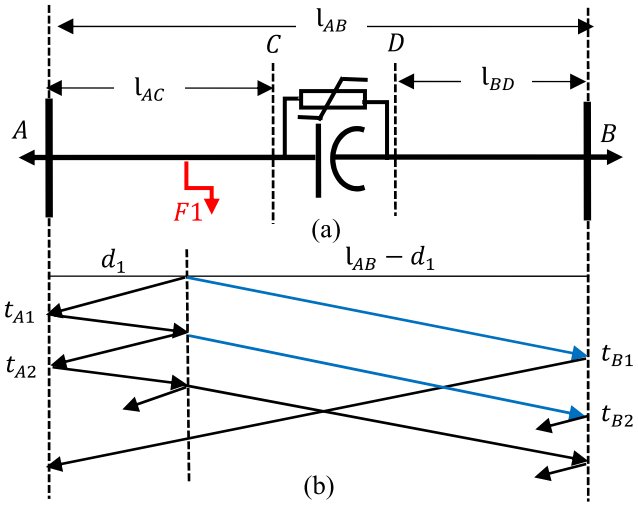

FIGURE 1. (a). Single line diagram of series compensated line and (b) lattice diagram for a fault in the left side of the compensator.

$$t_{A2} = t_{0A} + \frac{3\mathrm{d}_1}{v} \tag{2}$$

$$t_{B1} = t_{0B} + \frac{l_{\mathrm{AB}} - \mathrm{d}_1}{v} \tag{3}$$

$$t_{B2} = t_{0B} + \frac{l_{\mathrm{AB}} + \mathrm{d}_1}{v} \tag{4}$$

For the fault in the left side of the compensator, (1)-(4) provide the location

$$d_1 = [(t_{A2} - t_{A1}) + (t_{B2} - t_{B1})] \frac{l_{\mathrm{AB}}}{4(t_{B2} - t_{A1})} \tag{5}$$

where, t_{0A} and t_{0B} fault inception time at terminal A and B respectively, d_1 = fault distance from the terminal A for fault in the left side of the compensator and l_{AB} = length of the line.

2) FAULT ON THE RIGHT SIDE OF THE SERIES COMPENSATOR

Consider a fault in the second half-section ($l_{AB}/2 < d_2 < l_{AB}$) of the line and its lattice diagram as shown in Fig.2 (b).

From the diagram, we can write,

$$\mathrm{t_{A1}} = \mathrm{t_{0A}} + \frac{\mathrm{d}_2}{v} \tag{6}$$

$$\mathrm{t_{A2}} = \mathrm{t_{0A}} + \frac{2l_{\mathrm{AB}} - \mathrm{d}_2}{v} \tag{7}$$

$$t_{B1} = t_{0B} + \frac{l_{\mathrm{AB}} - \mathrm{d}_2}{v} \tag{8}$$

$$t_{B2} = t_{0B} + \frac{3(l_{\mathrm{AB}} - \mathrm{d}_2)}{v} \tag{9}$$

FL can be obtained using (6)-(9) for the fault in the right side of the compensator,

$$d_2 = l_{\mathrm{AB}} - [(t_{A2} - t_{A1}) + (t_{B2} - t_{B1})] \frac{l_{\mathrm{AB}}}{4(t_{A2} - t_{B1})} \tag{10}$$

where, d_2 = fault distance from the terminal A for the fault on the right side of the compensator.

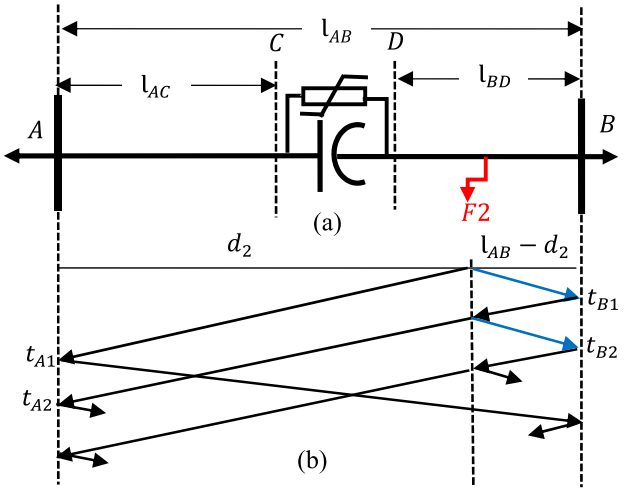

FIGURE 2. (a). Single line diagram of series compensated line and (b) lattice diagram for a fault in the right side of the compensator.

Two FLs d_1 and d_2 are calculated using (5) and (10) assuming the fault to be located on the left and right side of the compensator respectively. To select the correct FL out of these two values, we need to develop a faulted half-section identification (FHI) logic. The details are explained below.

B. PROPOSED FAULTED HALF-SECTION IDENTIFICATION LOGIC

In this section, we determine the FHI logic using the first two TW arrival times measured at the two terminals of the line. Consider the following two possible cases to determine the FHI logic.

Case 1: Consider fault on the left side of the compensator. From (1) - (4), we can calculate the two FHI indices,

$$FHI_{INDEX1} = t_{B2} - t_{A1} = l_{AB}/v \quad (11)$$

$$FHI_{INDEX2} = t_{A2} - t_{B1} = (4d_1 - l_{AB})/v \quad (12)$$

From (11) and (12), FHI_{INDEX1} (length of the line) is always greater than FHI_{INDEX2} (four times of d_1 minus length of the line) for the fault on the left side (first half-section of the line) of the compensator.

Case 2: Consider fault on the right side of the compensator from end-A. From (6)- (9), we have,

$$FHI_{INDEX1} = t_{B2} - t_{A1} = (3l_{AB} - 4d_2)/v \quad (13)$$

$$FHI_{INDEX2} = t_{A2} - t_{B1} = (l_{AB})/v \quad (14)$$

From (13) and (14), FHI_{INDEX1} (three times of the length of the line minus four times of d_2) is always less than FHI_{INDEX2} (length of the line) for the fault on the right side (second half-section of the line) of the compensator.

Special Case: Consider a fault at the midpoint of the line or on the compensator. The absolute differences between $(t_{B2} - t_{A1})$ and $(t_{A2} - t_{B1})$ is less than a threshold (e) then the faulted half-section is classified as the midpoint of the line or fault on the compensator. Then the final fault location estimate is the mean of the d_1 and d_2. The details of the algorithm steps are shown in Fig.3.

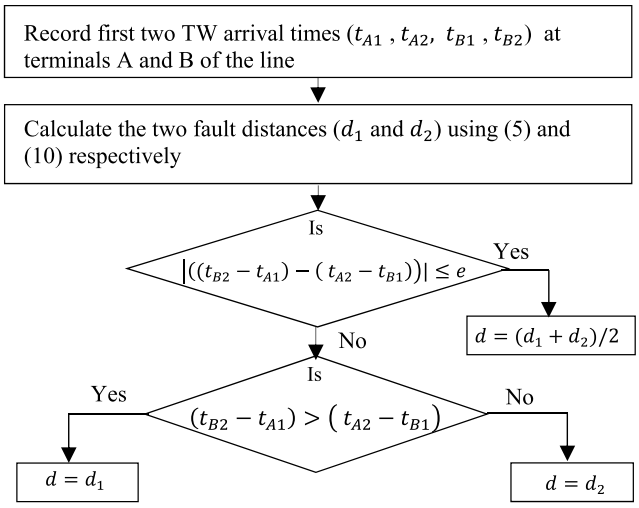

FIGURE 3. Flow diagram for the proposed method.

In this work, we used the threshold (e) and it is defined as 2μs for 1MHz sampling frequency implemented in the work. The threshold value is chosen based on the FL precision requirement which in turn depends on the sampling rate. For example, the accuracy that can be achieved with a 1MHz sampling rate is $\sim \pm 300$ meters (i.e. theoretically maximum possible error = wave speed x signal sampling frequency). This means a 1 μs (sampling interval) error in TW wavefront arrival time calculation can lead to an error of 300 meters assuming wave speed be approximately light speed. Considering a margin of two sample time error in TW arrival time estimation, we have chosen the value of the threshold is 2μs.

C. EFFECT OF LOCATION OF CAPACITOR AND LEVEL OF COMPENSATION ON FAULT LOCATION AND FHI

Series capacitors can be located anywhere on a transmission line. Series capacitors can be placed at one or both ends of a line as shown in Fig.4 (a) and (b) respectively, besides at the middle. Though the FL formulation is derived for the capacitor at the middle, the same analysis can be applied to the other configurations also. Further, the level of compensation does not affect the formulation [42] as evident in the above section. The FHI logic and analysis are also not affected by the position of the capacitor and level of compensation.

D. ILLUSTRATIVE ON APPLICATION OF THE PROPOSED METHOD

The proposed FL algorithm is explained here with an example on a 400-kV, 50 Hz, 300 km transmission line as in Fig.1(a) with 40% compensation at the middle (at l_{AC} =150km from terminal A). The source impedance and line configuration used for the PSCAD/EMTDC simulations are provided in the Appendix. The transmission line tower configuration used in the simulation is shown in Fig.10. Current signals are used for

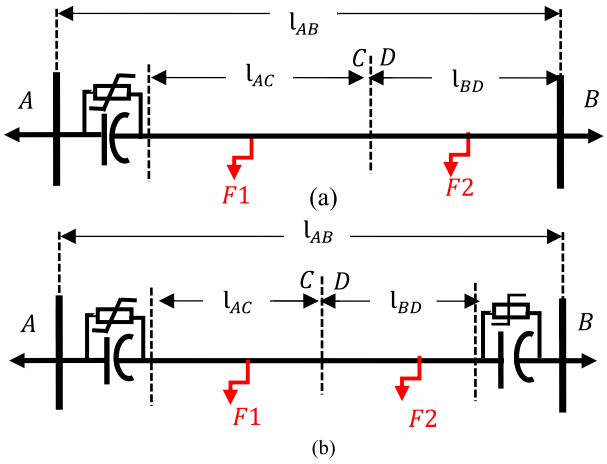

FIGURE 4. Single line diagram of series compensator at (a) one end and (b) both ends of the line.

TABLE 1. Three test scenarios to validate the proposed method.

Test scenario/ Parameters	A-g fault at 100km from Terminal A	AB fault at 150km from Terminal A	ABC-g fault at 250km from Terminal A
t_{A1} (μS)	346.00	518.00	862.00
t_{A2} (μS)	1033.00	1550.00	1205.00
t_{B1} (μS)	690.00	518.00	174.00
t_{B2} (μS)	1377.00	1549.00	518.00
d_1 (km)	**99.95**	**150.07**	-1549.78
d_2 (km)	-0.43	**150.07**	**250.02**
FHI_{INDEX1}	1031.00	1031.00	-344.00
FHI_{INDEX2}	343.00	1032.00	1031.00
FL (d) (km)	**99.95**	**150.07**	**250.02**
FL Error (%)	**0.01**	**0.02**	**0.01**

capturing TWs as current transformer [43] has the advantage of wider and flatter response and it is more consistent in TW detection [16]. The synchronized current signals are measured at the terminals A and B of the line at a sampling rate of 1MHz. The TWs are extracted using the bandpass filter and the arrival times of TWs are calculated using a parabola-based interpolation technique [16], which is robust and provides an accuracy of 0.5 μs at 1MHz sampling rate [16]. The wave speed is not required for this method. The FL, 'd' is calculated at terminal A and % error of FL is expressed as in (15)

$$\%\text{Error} = \left| \frac{\text{Actual FL} - \text{Calculated FL}}{\text{The total length of the line}} \right| \text{x100} \qquad (15)$$

For the illustration, a phase A-to-ground fault ($F1$) with a fault resistance of 50Ω and fault inception angle of 60^0, on the left side of the series compensator, at 100km from terminal A is considered. For this case, Fig.5 shows the first two TW arrival times measured at terminal A ($t_{A1} = 346$ and $t_{A2} = 1033$ μs) and terminal B ($t_{B1} = 690$ and $t_{B2} = 1377$ μs) of the line. The FL d_1 and d_2 calculated using (5) and (10) are 99.95km and -0.43km respectively. The calculated first FHI index using (11) ($FHI_{INDEX1} = 1031\mu$s) is greater than the second FHI index using (12) ($FHI_{INDEX2} = 343$ μs). Therefore, the fault is identified to be on the left side of the compensator (first half-section) and the final FL is 99.95km. The FL error calculated using (15) becomes 0.01%.

After estimating the FL accurately, wave speed can be calculated from $(l_{\text{AB}}/(t_{B2} - t_{A1}))$ and using FHI and FL values. The obtained wave speed for the system is 2.91715282×10^8m/s which matches to the actual wave speed (2.91698524×10^8m/s) as found from the parameters of the line. This wave speed can be used in setting traveling wave-based distance protection functions for the line.

Two other scenarios are used for the illustration and corresponding results are summarized in Table 1. It is noted that the highest error of FL is 0.024% (72 m) for the 300-km SCL. The illustration reveals that the proposed technique identifies FHI correctly and locates the fault accurately. The accuracy of the method is independent of FL and fault type.

III. RESULTS AND ANALYSIS

In this section, we provide results of detailed testing of the proposed FL method. Specifically, we carried out the following studies: (A) comparison with classical two-ended method, (B) performance analysis for fault inception close to voltage-zero-crossing, (C) study of the influence of fault resistance and fault type, (D) performance analysis under the influence of signal noise and sampling rate, (E) performance analysis for various locations of the series compensator, (F) comparative assessment with the model-free method and (G) validation with practical data (field record). The same test system as described in Section II (D) is used for studies Section III (A) to (F).

A. COMPARATIVE ASSESSMENT WITH COMMERCIALLY AVAILABLE CLASSICAL TWO-ENDED METHODS

The FL calculated by the commercially available classical two-ended methods [16], [17] needs wave speed of the line which depends on the line parameters. Any error in these parameters will affect the precision of the FL technique. Such inaccuracies may occur due to aging, temperature, sag of the conductor, etc., of the line. Several online parameter estimation methods are available which may not work for SCL due to non-linear characteristics of the MOV present in the measurement loop. In this section, we compare the proposed method with commercially established two-ended methods [16], [17]. For this purpose, we have considered phase-to-ground, phase-to-phase-ground, and 3-phase faults with an arc resistance of 100, 50, and 20Ω respectively. The fault inception angle (FIA) of 60^0 and different fault locations of 50, 150, and 250 km from terminal A of the line are considered. Accuracy of the proposed technique is assessed for different errors ranging from 0.5% to 20% of the wave speed. The evaluation results are provided in Table 2.

TABLE 2. Comparative assessment of the proposed method with commercially available two ended methods [16], [17].

Test cases	Two-ended method [16]-[17]			Proposed method	
	Wave speed Error (%)	FL (d) (km)	Error (%)	FL(d) (km)	Error (%)
A-g fault, R_F 100Ω, FIA 60^0 and FL 50km	0.0	50.03	**0.01**	49.97	**0.01**
	0.5	49.60	**0.13**	49.97	**0.01**
	1.0	49.10	**0.29**	49.97	**0.01**
	2.0	48.10	**0.64**	49.97	**0.01**
	5.0	45.12	**1.63**	49.97	**0.01**
	10.0	40.11	**3.29**	49.97	**0.01**
	15.0	35.14	**4.95**	49.97	**0.01**
	20.0	30.01	**6.64**	49.97	**0.01**
AB-g fault, R_F 50Ω, FIA 60^0 and FL 150km	0.0	150.07	**0.02**	150.07	**0.02**
	0.5	150.15	**0.04**	150.07	**0.02**
	1.0	150.21	**0.07**	150.07	**0.02**
	2.0	150.29	**0.09**	150.07	**0.02**
	5.0	150.44	**0.15**	150.07	**0.02**
	10.0	150.61	**0.21**	150.07	**0.02**
	15.0	150.97	**0.32**	150.07	**0.02**
	20.0	151.27	**0.42**	150.07	**0.02**
3-Phase fault, R_F 20Ω, FIA 60^0 and FL 250km	0.0	249.89	**0.03**	250.02	**0.01**
	0.5	250.61	**0.20**	250.02	**0.01**
	1.0	250.89	**0.29**	250.02	**0.01**
	2.0	251.89	**0.63**	250.02	**0.01**
	5.0	254.87	**1.63**	250.02	**0.01**
	10.0	259.88	**3.29**	250.02	**0.01**
	15.0	264.88	**4.96**	250.02	**0.01**
	20.0	269.87	**6.63**	250.02	**0.01**

For the classical double-ended methods [16], [17], FL error increases for higher errors in the wave speed which is an input to the algorithms. The FL error becomes 3.29% even with a 10% error in wave speed. The impact of wave speed (v) error on these methods is however less when the fault happens on the compensator or in the middle of the line. This is because in these classical methods the equation used for FL calculation is ($d = \frac{l_{AB}}{2} - (t_{B1} - t_{A1})v/2$) in which contribution of $\frac{l_{AB}}{2}$ the portion to final FL is more compared to contribution from $(t_{B1} - t_{A1})v/2$) portion. In contrast, the accuracy of the proposed method is better and consistent across the test scenarios as it does not dependent on the wave speed. Therefore, it can be concluded that the proposed method is more suitable for practical deployment for series compensated lines as for these lines online parameter computation is very challenging.

B. PERFORMANCE ANALYSIS FOR FAULT INCEPTION CLOSE TO VOLTAGE-ZERO-CROSSING

Faults occurring near voltage zero-crossing may subdue the TW magnitudes which also attenuate over long SCLs. Therefore, it is important to validate the proposed method under such conditions. Phase-to-ground and phase-to-phase faults with fault inception at voltage zero-crossing are considered for the study. Also, different R_F of 20, 50 Ω for phase-to-ground faults, and 10, 20Ω for phase-to-phase faults are used for simulations. Two FLs, one at 125 and the other at 275 km from the terminal of the line are simulated and the results are presented in Table 3. From the table, it can be seen that

TABLE 3. Study for fault inception at the near-zero crossing of the voltage.

Fault (%)	R_F (Ω) type	Actual	Calculated FL (km)	Error FL (km)
A-g	10.0	125	124.95	0.01
	10.0	275	275.06	0.02
	50.0	125	124.95	0.01
	50.0	275	275.06	0.02
AB	5.0	125	124.87	0.04
	5.0	275	275.07	0.02
	20.0	125	124.87	0.04
	20.0	275	275.07	0.02

the proposed method can locate faults accurately in these conditions.

C. STUDY OF THE INFLUENCE OF FAULT RESISTANCE AND FAULT TYPE

Various fault types with the variation of fault R_F are simulated FL at 275km from terminal A. The R_F of each fault type is varied from 0.1 to 100Ω. The results for the proposed method and classical methods [16], [17] are listed in Table 4. It is observed that the proposed method provides accurate results even for high R_F, while the classical methods show more error for the remote fault. This is due to TWs dispersion effect [37], [38] which is being mitigated in the proposed method.

TABLE 4. Study of the influence of fault resistance and fault type.

Fault Type	Fault location estimation error (%)					
	A-g		AB		ABC-g	
R_F (Ω)	[16]-[17]	Proposed	[16]-[17]	Proposed	[16]-[17]	Proposed
0.1	0.086	0.045	0.284	0.108	0.081	0.054
10	0.086	0.045	0.283	0.108	0.081	0.054
50	0.086	0.045	0.288	0.106	0.081	0.054
100	0.092	0.045	0.288	0.106	0.081	0.054

D. PERFORMANCE ANALYSIS UNDER THE INFLUENCE OF SIGNAL NOISE AND SAMPLING RATE

The performance of TW based FL methods depends on the signal sampling rate and measurement noise. In this study, we tested the proposed method with different levels of noise in the current signal under varying sampling rates. A total of 560 fault conditions are simulated and tested. The method is robust against noise and sampling rate. The summary of the considered fault scenarios is tabulated in Table 9 in the Appendix. The results are provided in Table 5. The results show that the proposed method can calculate the FL accurately with an average and maximum errors of 0.07% and

TABLE 5. Study of signal noise and Sampling rate on the FL precision.

Sampling Frequency	Fault location estimation error (%)							
	No noise		0.5% noise		1% noise		2% noise	
	Avg.	Max.	Avg.	Max.	Avg.	Max.	Avg.	Max.
500kHz	0.08	0.38	0.12	0.71	0.14	0.63	0.45	1.89
1MHz	0.04	0.11	0.09	0.29	0.07	0.37	0.12	0.91
2MHz	0.03	0.08	0.07	0.18	0.06	0.24	0.09	0.87

0.37% respectively for the signal noise of 1% and a sampling rate of 1MHz. The accuracy of TW based FL depends on the TW time of arrival estimation [16], [24]. In the proposed method, an advanced interpolation algorithm is used for TW time of arrival estimation. It is also observed that errors are noticeable when the method is implemented with lower sampling rates, and when the noise level is more than 1%. This is because the technique is unable to calculate accurate second TW arrival time for close-in faults. The proposed method is precise, and FL accuracy can be achieved within a two-tower span (280-320m) distance using 1MHz sampling rate.

E. EFFECT OF LOCATION OF THE SERIES COMPENSATOR

In this section, we tested the method for (i) compensator at one end with a 50% of the fixed compensation and (ii) compensator at both ends of the line with a 70% fixed compensation as shown in Fig.4. Various fault types with the variation of R_F are simulated at FL of 125km from terminal A. The R_F of each fault type is varied from 0.1 to 50 Ω. The results for the proposed method are listed in Table 6. From the table, it is evident that the accuracy of the method is not affected by the location and compensation level of the compensator.

TABLE 6. Study of the influence of compensator location.

Fault Type	Fault location estimation error (%)					
	A-g		AB		ABC-g	
R_F (Ω)	FSC at one end	FSC at two ends	FSC at one end	FSC at two ends	FSC at one end	FSC at two ends
0.1	0.045	0.045	0.106	0.108	0.061	0.054
10	0.046	0.045	0.106	0.108	0.061	0.054
50	0.046	0.045	0.106	0.106	0.061	0.054

F. COMPRATIVE ASSESSMENT WITH MODEL-FREE METHOD

In this section, the performance of the proposed method is compared with the model-free technique of [36]. This is a search-based method and depends on the time difference between the first incident TW and the one reflection from the fault point, at both terminals of the line. Two cases (F1 and F2) for analysis are simulated. For Case 1, a phase

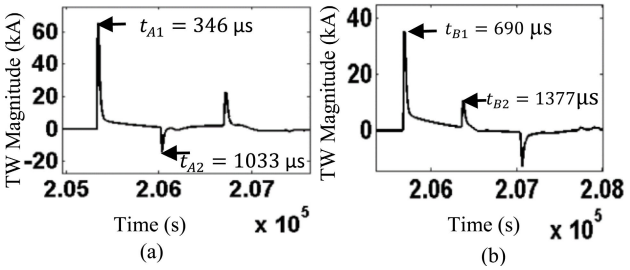

FIGURE 5. TW arrival times measured at (a) terminal A and (b) terminal B for a fault at 100km from terminal A of the line.

A-to-ground fault ($F1$) with $R_F = 50\Omega$ and FIA of 60^0, FL at 125km from terminal A is considered. For this case, Fig.6 (a) shows lattice diagram and Fig.6 (b) provides the first two TW arrival times measured at terminal A ($t_{A1} = 432$ and $t_{A2} = 1290$ μs) and terminal B ($t_{B1} = 604$ and $t_{B2} = 1362$ μs) of the line. The calculated FLs using the method [36] and the proposed method are 125.12 and 124.951km (corresponding %FL error 0.04 and 0.016) respectively. Here, arrival times of fault point reflection at terminal A and B are measured $t_{A2} = 1290\mu$s and $t_{B3} = 1805\mu$s respectively for the method [36].

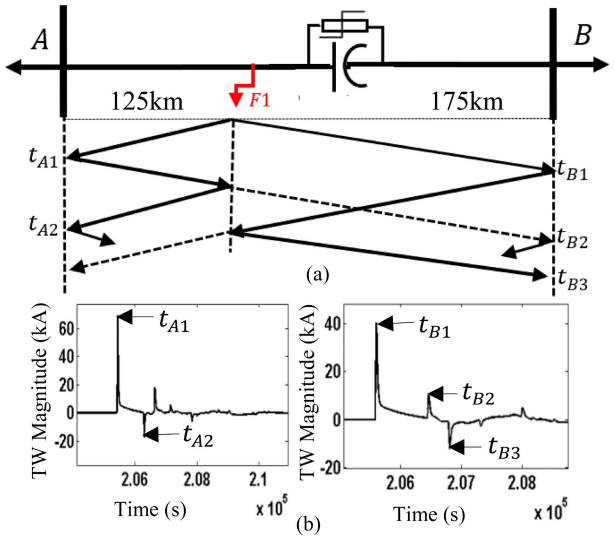

FIGURE 6. (a) Lattice diagram and (b) TW arrival times measured at terminal A and terminal B for Case 1.

For Case 2, a phase A-to-ground fault ($F2$) with $R_F = 20\Omega$ and FIA of 90^0 at 275km from terminal A is simulated. For this case, Fig.7 (a) shows the lattice diagram and corresponding first two TW arrival times measured at terminal A ($t_{A1} = 947$ and $t_{A2} = 1119\mu$s) and terminal B ($t_{B1} = 88$ and $t_{B2} = 260$ μs) of the line are shown in Fig.7 (b).

From the lattice diagram, 12th reflection is the fault point reflection from terminal A and it is required for the method [36]. The 12th TW reflection is attenuated and therefore not possible to capture its arrival time reliably. The method [36] is not able to calculate the FL for Case 2. The proposed method requires only the first two TW arrival times at both the terminals of the line and the calculated FL and %FL error using the proposed method are 274.975 and

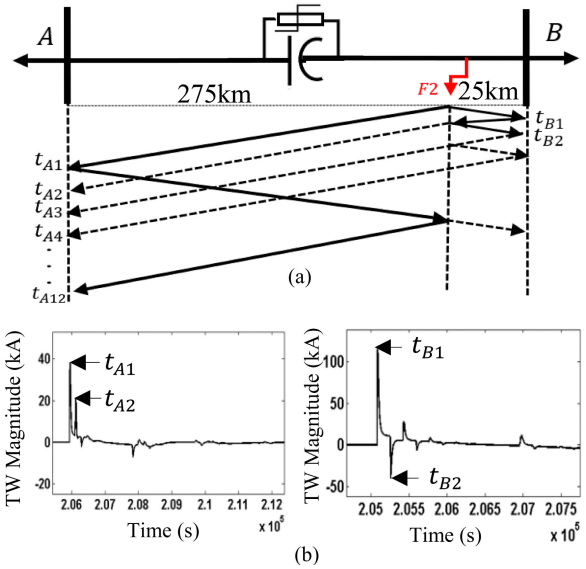

FIGURE 7. (a) Lattice diagram and (b) TW arrival times measured at terminal A and terminal B for Case 2.

0.008 respectively for this case. The method [36] finds limited performance for faults close to the terminals of the line due to the requirement of TW arrival times of incident and reflection waves from the fault point, at both ends.

G. VALIDATION WITH PRACTICAL DATA

In this section, the proposed method is validated with field data from a double circuit SCL [40], [41] in Indian Power Grid between Jeypore-Gazuwaka as shown in Fig.8. FSC is placed at Jeypore 400-kV substation end with 50% fixed compensation. The total length of the line is 225km and the current signal is measured before the FSC at Jeypore end and Gazuwaka end with a sampling rate of 5MHz sampling [17].

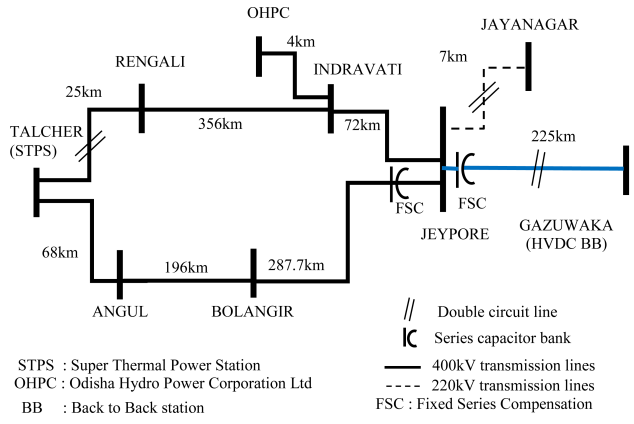

FIGURE 8. Jeypore-Gazuwaka 400-kV double circuit series compensated line in Indian Power Grid.

A phase-B-to-ground fault occurred on March 19, 2020, on Jeypore-Gazuwaka line-1. Fig.9 shows the TWs captured at Jeypore and Gazuwaka terminals for the fault and TW arrival times are marked in the figure. The TW arrival times obtained from the disturbance records are listed in Table 7.

TABLE 7. First two TW arrival time recorded at both the terminals.

Terminal Name	First arrival time (s)	Second arrival time (s)
Jeypore-end (t_J)	29.849895	29.850231
Gazuwaka-end (t_G)	29.849463	29.849806

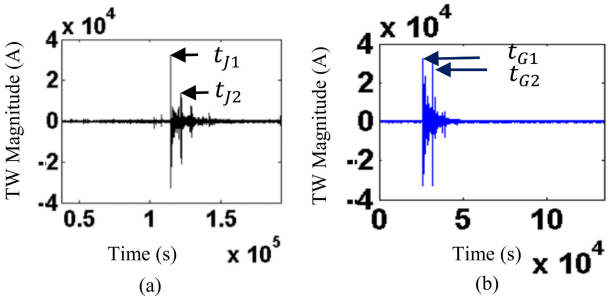

FIGURE 9. TWs recorded at (a) Jeypore terminal and (b) Gazuwaka terminal for Phase-B-to-ground fault at 175.12km of the line from Jeypore end.

Based on the recorded TW arrival times, the FL d_1 and d_2 calculated using (5) and (10) are -429.123km and 175.268km respectively. The calculated first FHI index ($FHI_{INDEX1} = -89\ \mu s$) is less than the second FHI index ($FHI_{INDEX2} = 768\ \mu s$). Therefore, the fault is classified to be on the second half-section of the line. The final FL is found to be 175.268 km from Jeypore end. The actual fault location identified by the substation staff is 175.12 km from the Jeypore end. The FL error calculated using (15) becomes 0.065%. The calculated wave speed is $2.92968749X10^8$m/s. This field case demonstrated that the proposed method can locate the fault within a two-tower span distance without using wave speed.

IV. CONCLUSION

In this work, a simple *model-free* TW based FL method for a series compensated line is presented. The first two TW arrival times from both terminals are the only inputs to the fault locator. The wave speed, parameters of the line, or the series compensator are not required to be known. A precise faulted half-section identification logic, with respect to the compensator, is developed using the first two TWs measured at both terminals which facilitates the selection of the correct fault distance out of the two estimates. Simulation results show that the performance of the method for series compensated line is accurate for various fault scenarios. The accuracy of the method is compared to a commercially available classical two-terminal methods [16], [17] for error in wave speed of the line. For the classical methods, the FL error increases for higher inaccuracies in wave speed whereas, the proposed method is independent of the wave speed. The proposed method is also compared with the available setting-free method and performance is superior for the faults close to the terminals.

The method is also tested for various fault scenarios and locations of the compensator. The simulation studies reveal

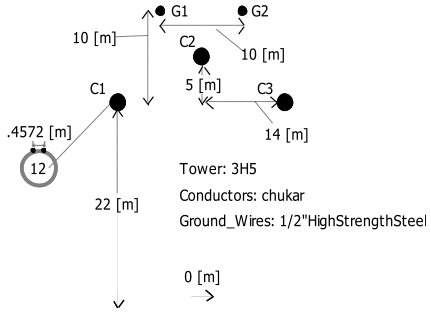

FIGURE 10. Tower configuration for the simulated transmission line.

TABLE 8. Source impedances.

Sequence	Terminal A-end	Terminal B-end
Positive	0.8703+36.247 Ω	1.6531+44.546 Ω
Negative	0.8703+36.247 Ω	0.6531+44.546 Ω
Zero	3.2874+39.826 Ω	7.1734+44.546 Ω

TABLE 9. Fault cases considered for the test system.

Test cases	Test conditions
FL (km)	5, 50, 100, 150, 200, 250 and 295
Type of fault	a-g, a-b, c-a-g and a-b-c-g
FIA (degree)	0, 60, 135, 150 and 180
Arc resistance (Ω)	0.01, 10, 50, and 100

that it is possible to achieve FL precision of ± 300m using 1MHz sampling frequency. The proposed method is also validated with field recorded data from a series compensated line in Indian Power grid with an accuracy of a tower span. The technique can be implemented in IEDs with a 1MHz sampling rate to achieve FL precision of two tower span distance.

The proposed method being free of the wave speed as an input, does not necessitate field experiments or accurate line parameters to obtain the same which is required in many available methods. Any pre-defined setting is not required and is cost-effective for practical deployment. The proposed model-free approach is an attractive option to be incorporated in control centers or cloud-based systems. Further, the wave speed of the line can be calculated using the obtained fault location information for other power system protection and monitoring applications.

APPENDIX

See Figure 10 and Tables 8 and 9.

ACKNOWLEDGMENT

The authors express gratitude to Eastern Region Load Dispatch Center (ERLDC), India, and POWERGRID, India for sharing system data, disturbance recorder data for academic and research purposes.

REFERENCES

[1] CIGRE Working Group. (2010). *Protection, Control and Monitoring of Series Compensated Networks, e-CIGRE*. [Online]. Available: https://e-cigre.org/publication/411-protection-control-and-monitoring-of-series-compensated-networks

[2] K. Bogdan, "Distance protection of series compensated lines-problems and solutions," in *Proc. 27th Annu. Western Protective Relay Conf.*, 2001, pp. 22–25.

[3] R. Dubey, S. R. Samantaray, B. K. Panigrahi, and V. G. Venkoparao, "Koopman analysis based wide-area back-up protection and faulted line identification for series-compensated power network," *IEEE Syst. J.*, vol. 12, no. 3, pp. 2634–2644, Sep. 2018.

[4] M. M. Saha, J. Izykowski, and E. Rosolowski, *Fault Location on Power Networks* (Power Systems). London, U.K.: Springer, 2010.

[5] *IEEE Guide for Determining Fault Location on AC Transmission and Distribution Lines*, IEEE Standard C37.114-2014 (Revision of IEEE Std C37.114-2004), Jan. 2015, pp. 1–76.

[6] S. Das, S. Santoso, A. Gaikwad, and M. Patel, "Impedance-based fault location in transmission networks: Theory and application," *IEEE Access*, vol. 2, pp. 537–557, May 2014.

[7] A. L. Dalcastagne and S. L. Zimath, "A study about the sources of error of impedance-based fault location methods," in *Proc. IEEE/PES Transmiss. Distrib. Conf. Expo., Latin Amer.*, Bogota, Colombia, Aug. 2008, pp. 1–6.

[8] J. Izykowski, E. Rosolowski, P. Balcerek, M. Fulczyk, and M. M. Saha, "Fault location on double-circuit series-compensated lines using two-end unsynchronized measurements," *IEEE Trans. Power Del.*, vol. 26, no. 4, pp. 2072–2080, Oct. 2011.

[9] T. P. S. Bains and M. R. D. Zadeh, "Supplementary impedance-based fault-location algorithm for series-compensated lines," *IEEE Trans. Power Del.*, vol. 31, no. 1, pp. 334–342, Feb. 2016.

[10] S. Gajare and A. K. Pradhan, "An accurate fault location method for multi-circuit series compensated transmission lines," *IEEE Trans. Power Syst.*, vol. 32, no. 1, pp. 572–580, Jan. 2017.

[11] N. Kang, J. Chen, and Y. Liao, "A fault-location algorithm for series-compensated double-circuit transmission lines using the distributed parameter line model," *IEEE Trans. Power Del.*, vol. 30, no. 1, pp. 360–367, Feb. 2015.

[12] Y. Zhang, J. Liang, Z. Yun, and X. Dong, "A new fault-location algorithm for series-compensated double-circuit transmission lines based on the distributed parameter model," *IEEE Trans. Power Del.*, vol. 32, no. 6, pp. 2398–2407, Dec. 2017.

[13] T. P. S. Bains, T. S. Sidhu, Z. Xu, I. Voloh, and M. R. D. Zadeh, "Impedance-based fault location algorithm for ground faults in series-capacitor-compensated transmission lines," *IEEE Trans. Power Del.*, vol. 33, no. 1, pp. 189–199, Feb. 2018.

[14] R. Rubeena, M. R. D. Zadeh, and T. P. S. Bains, "An accurate offline phasor estimation for fault location in series-compensated lines," *IEEE Trans. Power Del.*, vol. 29, no. 2, pp. 876–883, Apr. 2014.

[15] T. P. S. Bains and M. R. D. Zadeh, "Enhanced phasor estimation technique for fault location in series-compensated lines," *IEEE Trans. Power Del.*, vol. 30, no. 4, pp. 2058–2060, Aug. 2015.

[16] E. O. Schweitzer, A. Guzman, M. V. Mynam, V. Skendzic, B. Kasztenny, and S. Marx, "Locating faults by the traveling waves they launch," in *Proc. 67th Annu. Conf. Protective Relay Eng.*, Mar. 2014, pp. 95–110.

[17] *Reason RPV311 Digital Fault Recorder With Fault Location and PMU*. Accessed: Oct. 2015. [Online]. Available: https://www.gegridsolutions.com/publications/GridSolutionsBrochures/Grid-SAS-L3-REASON_RPV311-0889-2015_10-EN.pdf

[18] D. J. Spoor, J. Zhu, and P. Nichols, "Single-ended traveling wave based fault location on two terminal transmission lines," in *Proc. IEEE TENCON Conf.*, Singapore, Jan. 2010, pp. 1–4.

[19] A. Guzman, B. Kasztenny, Y. Tong, and M. V. Mynam, "Accurate and economical traveling-wave fault locating without communications," in *Proc. 71st Annu. Conf. Protective Relay Eng. (CPRE)*, College Station, TX, USA, Mar. 2018.

[20] R. Razzaghi, G. Lugrin, H. Manesh, C. Romero, M. Paolone, and F. Rachidi, "An efficient method based on the electromagnetic time reversal to locate faults in power networks," *IEEE Trans. Power Del.*, vol. 28, no. 3, pp. 1663–1673, Jul. 2013.

[21] M. Korkali, H. Lev-Ari, and A. Abur, "Traveling-wave-based fault-location technique for transmission grids via wide-area synchronized voltage measurements," *IEEE Trans. Power Syst.*, vol. 27, no. 2, pp. 1003–1011, May 2012.

[22] D. Tzelepis, A. Dysko, C. Booth, G. Fusiek, P. Niewczas, and T. C. Peng, "Distributed current sensing technology for protection and fault location applications in high-voltage direct current networks," *J. Eng.*, vol. 2018, no. 15, pp. 1169–1175, Oct. 2018.
[23] F. V. Lopes, K. M. Silva, F. B. Costa, W. L. A. Neves, and D. Fernandes, "Real-time traveling-wave-based fault location using two-terminal unsynchronized data," *IEEE Trans. Power Del.*, vol. 30, no. 3, pp. 1067–1076, Jun. 2015.
[24] O. Naidu and A. K. Pradhan, "A traveling wave-based fault location method using unsynchronized current measurements," *IEEE Trans. Power Del.*, vol. 34, no. 2, pp. 505–513, Apr. 2019.
[25] F. V. Lopes, P. Lima, J. P. G. Ribeiro, T. R. Honorato, K. M. Silva, E. J. S. Leite, W. L. A. Neves, and G. Rocha, "Practical methodology for two-terminal traveling wave-based fault location eliminating the need for line parameters and time synchronization," *IEEE Trans. Power Del.*, vol. 34, no. 6, pp. 2123–2134, Dec. 2019.
[26] Y. Liu, S. Meliopoulos, N. Tai, L. Sun, and B. Xie, "Protection and fault locating method of series compensated lines by wavelet based energy traveling wave," in *Proc. IEEE Power Energy Soc. Gen. Meeting*, Chicago, IL, USA, Jul. 2017, pp. 1–5.
[27] B. Sahoo and S. R. Samantaray, "An enhanced travelling wave-based fault detection and location estimation technique for series compensated transmission network," in *Proc. 7th Int. Conf. Power Syst. (ICPS)*, Pune, India, Dec. 2017, pp. 61–68.
[28] M. Abedini, A. Hasani, A. H. Hajbabaie, and V. Khaligh, "A new traveling wave fault location algorithm in series compensated transmission line," in *Proc. 21st Iranian Conf. Electr. Eng. (ICEE)*, Mashhad, Iran, May 2013, pp. 1–6.
[29] A. Momen, Y. Chakhchoukh, and B. K. Johnson, "Series compensated line parameters estimation using synchrophasor measurements," *IEEE Trans. Power Del.*, vol. 34, no. 6, pp. 2152–2162, Dec. 2019.
[30] S. G. Srivani and K. Panduranga Vittal, "Adaptive distance relaying scheme in series compensated transmission lines," in *Proc. Joint Int. Conf. Power Electron., Drives Energy Syst. Power India*, Dec. 2010, pp. 1–7.
[31] E. O. Schweitzer, M. V. Mynam, A. Guzman-Casillas, V. Skendzic, B. Z. Kasztenny, and D. E. Whitehead, "Power line parameter adjustment and fault location using traveling waves," U.S. Patent 8 990 036 B1, Mar. 24, 2015.
[32] O. D. Naidu, N. George, and P. Yalla, "Setting-free fault section identification and fault location method for three-terminal lines," in *Proc. 9th Int. Conf. Power Energy Syst. (ICPES)*, Perth, WA, Australia, Dec. 2019, pp. 1–6.
[33] A. G. Augustine and O. D. Naidu, "A novel fault section identification algorithm for a series-compensated transmission line," in *Proc. 8th Int. Conf. Power Syst. (ICPS)*, Jaipur, India, Dec. 2019, pp. 1–6.
[34] F. V. Lopes, "Settings-free traveling-wave-based Earth fault location using unsynchronized two-terminal data," *IEEE Trans. Power Del.*, vol. 31, no. 5, pp. 2296–2298, Oct. 2016.
[35] J. Ding, L. Li, Y. Zheng, C. Zhao, H. Chen, and X. Wang, "Distributed travelling-wave-based fault location without time synchronisation and wave velocity error," *IET Gener., Transmiss. Distrib.*, vol. 11, no. 8, pp. 2085–2093, Jun. 2017.
[36] F. V. Lopes, K. M. Dantas, K. M. Silva, and F. B. Costa, "Accurate two-terminal transmission line fault location using traveling waves," *IEEE Trans. Power Del.*, vol. 33, no. 2, pp. 873–880, Apr. 2018.
[37] J. Qin, X. Chen, and J. Zheng, "Study on dispersion of travelling wave in transmission line," *Proc. Chin. Soc. Electr. Eng.*, vol. 19, no. 9, pp. 27–35, 1999.
[38] H. Jia, "An improved traveling-wave-based fault location method with compensating the dispersion effect of traveling wave in wavelet domain," *Math. Problems Eng.*, vol. 2017, Feb. 2017, Art. no. 1019591.
[39] T.-C. Lin, J.-Z. Yang, C.-S. Yu, and C.-W. Liu, "Development of a transmission network fault location platform based on cloud computing and synchrophasors," *IEEE Trans. Power Del.*, vol. 35, no. 1, pp. 84–94, Feb. 2020.
[40] R. K. Pandey, S. K. Soonee, L. Hari, P. Mukherjee, and S. Benerjee, "Study of HVDC system in open access—An Indian system experience," in *Proc. 16th Nat. Power Syst. Conf. (NPSC)*, Dec. 2010, pp. 109–114.
[41] J. L. N. Rao, G. Bansal, S. Auddy, T. Tulkiewicz, and M. Ohrstrom, "Mitigation of ferroresonance in line commutated HVDC converter interconnected with series compensated overhead line transmission system," in *Proc. IEEE Electr. Power Energy Conf. (EPEC)*, Ottawa, ON, Canada, Oct. 2016, pp. 1–6.
[42] S. Gajare, A. K. Pradhan, and V. Terzija, "A method for accurate parameter estimation of series compensated transmission lines using synchronized data," *IEEE Trans. Power Syst.*, vol. 32, no. 6, pp. 4843–4850, Nov. 2017.
[43] *ABB Instrument Transformers of IMB245 Technical Specifications*. Accessed: Mar. 2008. [Online]. Available: https://library.e.abb.com/public/1b61a98abcb38abec1257b130057b777/Buyers%20Guide%20Outdoor%20Instrument%20Transformers%20Ed%205%20en.pdf

O. D. NAIDU (Senior Member, IEEE) received the M.Tech. degree in power systems engineering from the Indian Institute of Technology (IIT), Kharagpur, India, in 2008, where he is currently pursuing the Ph.D. degree in electrical engineering. From 2009 to 2012, he was a Senior Power System Application Development Engineer with ABB GISPL, Bengaluru, India. From 2012 to 2019, he was a Principal Scientist with the ABB Corporate Research Center, Bengaluru. He is also working as a Senior Principal Engineer with the Hitachi ABB Power Grids Research and Development Center, Bengaluru. He is the author of more than 30 scientific papers and patent applications. His research interests include power system protection, fault location, renewable integration and monitoring, and artificial intelligence applications to power system protection and monitoring.

ASHOK KUMAR PRADHAN (Senior Member, IEEE) received the Ph.D. degree in electrical engineering from Sambalpur University, Sambalpur, India, in 2001. From 1992 to 2002, he was with the Department of Electrical Engineering, Veer Surendra Sai University of Technology, Burla, India. Since 2002, he has been with the Department of Electrical Engineering, Indian Institute of Technology, Kharagpur, India, where he is currently a Professor. His research interests include power system relaying and monitoring. He is a Fellow of the Indian National Academy of Engineering, India, and the National Academy of Sciences, India.